Journal of African Earth Sciences 173 (2021) 104051

Contents lists available at ScienceDirect

Journal of African Earth Sciences

journal homepage: www.elsevier.com/locate/jafrearsci

Towards a homogeneous moment magnitude determination for earthquakes in South Africa: Reduction of associated uncertainties

B. Manzunzu [a,b,*], M.B.C. Brandt [a], V. Midzi [a,b], R.J. Durrheim [b], I. Saunders [a], T.F. Mulabisana [a]

[a] Engineering and Geohazards, Council for Geoscience, South Africa
[b] School of Geosciences, University of the Witwatersrand, South Africa

ARTICLE INFO

Keywords:
Moment magnitude
Local magnitude
South Africa
Catalogue
Uncertainties
Orthogonal regression

ABSTRACT

New M_W–M_L magnitude relations valid for the periods January 1971–March 1997, April 1997–September 2012 and October 2012–present are presented for South Africa. Three M_W–M_L relations were derived for the respective periods by applying a general orthogonal regression using 85 mining-related and tectonic events. Moment magnitudes (M_W) were calculated using spectral analysis of the vertical component seismograms. A Brune model for source radiation was assumed. Attenuation functions previously derived from local seismic events were used. For each event, the final M_W was computed by taking the average of the values determined at four or more stations. These M_W values were used to compute new M_W –M_L regression equations for three previous M_L relations that had been used to compile the South African earthquake catalogue. The new M_W–M_L relations were then compared with the M_W determined from the Harvard Centroid Moment Tensor (CMT) project. The M_W computed using the relation derived for the most recent period (October 2012–present) produces M_W values that are similar to those reported by the Harvard CMT solutions. The relations can be used in the homogenization of the South African earthquake catalogue. Application of the new relations for the three periods will reduce uncertainty in the homogenized catalogues, which are important when calculating seismic hazard parameters (i.e. when estimating activity rates, b-values and M_{max}).

1. Introduction

Earthquake magnitude is a fundamental source parameter that allows scientists and civil authorities to estimate the severity of the ground motion resulting from earthquakes and its potential to cause damage to buildings and other critical structures, such as bridges and dams. Magnitude is also of primary importance in seismic hazard assessments and other seismicity studies (Gutenberg and Richter, 1944). Over the last hundred years, several magnitude scales have been proposed, for example local magnitude (M_L), body wave magnitude (m_B), surface wave magnitude (M_S) and moment magnitude (M_W); with each of these having its own advantages and disadvantages (Hanks and Kanamori, 1979; Lay and Wallace, 1995; Bormann, 2012). Each scale was determined for a specific frequency range and wave type and adjusted to match another scale at a certain range of magnitude (Kanamori, 1983, Table 1). Consequently, a given earthquake may be characterized by several different magnitude values determined by the same or different agencies, introducing significant uncertainty when assessing seismic hazard. Apart from M_W, the other magnitude scales saturate for large earthquakes. However, these magnitude scales continue to be used to estimate the magnitude values of frequently occurring small to moderate earthquakes in many different regions (cf. Biswas and Aki, 1984; Castellaro et al., 2006; Das et al., 2012; Gasperini et al., 2015; Saunders et al., 2013). Seismic hazard analysis requires a homogeneous catalogue (i.e. one that uses only one type of magnitude) with M_W having become the global standard (e.g. Stucchi et al., 2013; Di Giacomo et al., 2015; Burton et al., 2004; Kadirioğlu et al., 2018; Hussein et al., 2008). Consequently, magnitude scales should be converted to M_W, especially when merging two or more catalogues with different magnitude scales.

With Aki's (1966) introduction of the concept of seismic moment (M_0), a physically meaningful measure of the strength of a general seismic source was created. The moment magnitude scale (M_W) was developed thus solving the problem of magnitude saturation (Hanks and Kanamori, 1979). Ideally, M_W can be calculated for all earthquakes from micro to mega earthquakes. However, owing to high noise in lower-magnitude earthquakes, especially for regional networks, it is very difficult to determine the corner frequency. Hence M_W is generally calculated for earthquakes of magnitude 4 and above. Although the

* Corresponding author. Engineering and Geohazards, Council for Geoscience, South Africa.
E-mail address: bmanzunzu@geoscience.org.za (B. Manzunzu).

https://doi.org/10.1016/j.jafrearsci.2020.104051
Received 26 May 2020; Received in revised form 13 August 2020; Accepted 19 October 2020
Available online 25 October 2020
1464-343X/

Table 1
Different magnitude scales used for quantifying earthquake size and their periods of validity (modified from Kanamori, 1983).

Magnitude scale name	Designation	Phase on which window is selected for measurement (e.g. P- or S-waves)	Period of validity	Related magnitude scale
Local	M_L	Largest amplitude on the Wood-Anderson seismogram	0.1–3 s	M_{blg} (Nuttli, 1973)
Surface wave	M_S	Surface waves	~20 s	$M_S \approx M_L$ at $M \approx 6$
Body wave	m_B	Body waves (P, PP and S phases)	0.5–12 s	$M_B \approx M_S$ for $6.5<M<7$
Moment	M_W	Body waves (P and S phases)	10–∞ seconds	M_L, M_S, m_B

determination of M_W is not a straightforward method for routine use, especially for small-magnitude earthquakes, the method is widely used in modern seismotectonic research and seismic hazard analysis where large earthquake magnitudes play a pivotal role (Brandt and Saunders, 2011). For regional earthquakes, the simplest way to determine M_W is through spectral analysis of either P- or S-waves. This is often the only reliable technique, since the low frequencies needed for a stable inversion are difficult to obtain for smaller events from seismograms recorded by regional networks, owing to attenuation (Brandt and Saunders, 2011).

The most common magnitude used worldwide is the local magnitude scale mainly because it is quick and easy to compute and can be used for small to moderately sized seismic events. M_L depends on the local attenuation function; therefore, it is region dependent. In this regard, a single earthquake may have different M_L values derived from different attenuation relations for different regions. The South African National Seismograph Network (SANSN), established in 1970, has used several M_L relations over time to quantify the sizes of earthquakes. This has created a heterogeneous earthquake catalogue in terms of the magnitude values. Initially, the SANSN magnitude determinations were based on the local magnitude equation modified by Fernandez (1980) from the Richter equation:

$$M_L = \log_{10}\left(\frac{A_V}{T}\right) + 0.84\log_{10}\triangle + 1.26 \quad (1)$$

where Δ (in degrees) is the epicentral distance and T (s) is the peak-to-peak period. Strictly speaking, this formula (Equation (1)) is only applicable to horizontal components measured on a Wood-Anderson seismograph, while the SANSN mostly used short-period vertical component instruments (Brandt, 1997; Saunders et al., 2013). Such a situation was also common in other regions of low seismicity prior to the derivation of locally calibrated M_L scales (Greenhalgh and Singh, 1986; Kim, 1998; Muço et al., 2002).

Beginning in 1997, the SANSN upgraded from analogue to digital seismometry, heralding the introduction of a new local magnitude relation, which was a modification of the Hutton and Boore (1987) equation:

$$M_L = 1.10\log_{10}\left(\frac{r}{100}\right) + 0.00189(r-100) + \log_{10} A + 3 + S \quad (2)$$

where r (km) is the epicentral distance, S is the station correction term and A (mm) is the maximum amplitude on the vertical component.

Since 2012, an M_L scale calibrated using a selection of high-quality local recordings of tectonic events recorded at a minimum of five stations is being used (Saunders et al., 2013), and is shown in Equation (3).

$$M_L = 1.149\log_{10}(R) + 0.00063R + \log_{10}(A) - 2.04 + S \quad (3)$$

where A (nm) is the maximum amplitude of the S/Lg phase on the

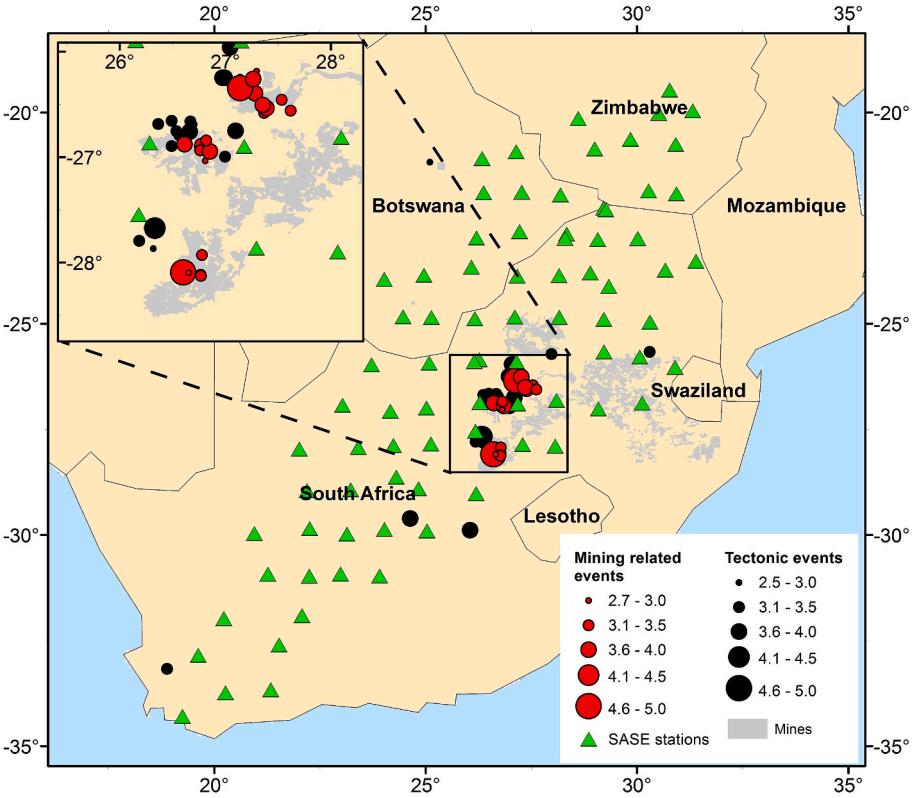

Fig. 1. Seismological stations of the SASE project shown as green triangles. The circles represent the locations of the epicentres of the seismic events used in this study (red circles indicate mining-related events, while black circles denote tectonic events). The classification is based on the proximity of the event to the mining boundaries. (For interpretation of the references to colour in this figure legend, the reader is referred to the Web version of this article.)

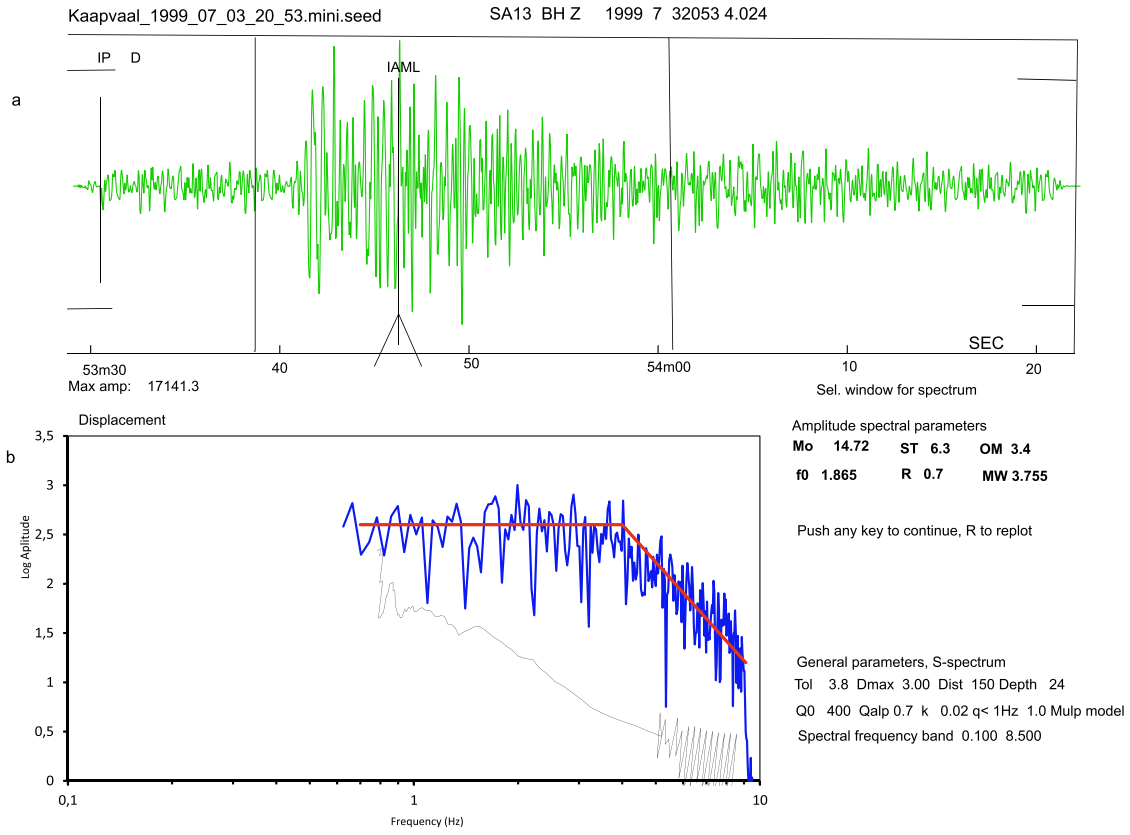

Fig. 2. (a) Example of a typical waveform used in the determination of M_W for station SA13. The vertical component seismogram with the time window used for spectral analysis is shown. The amplitude phase is represented by IAML; the P- phase is IP and the polarity D. The window between 53m38s and 54m02s represents the window selected for the spectral inversion. b) The displacement spectrum (solid black line) obtained from the window is shown in (a) with the noise spectrum represented by a grey line. The moment magnitude was calculated for the corresponding displacement spectra, with the flat portion at low frequencies. The spectral parameters determined for this event are shown in (b) as the seismic moment (M_0) in dynes, the stress drop (ST) in bars, the flat spectral level (OM), the corner frequency (f0) in Hertz, the source radius (R) in kilometres and the moment magnitude (M_W).

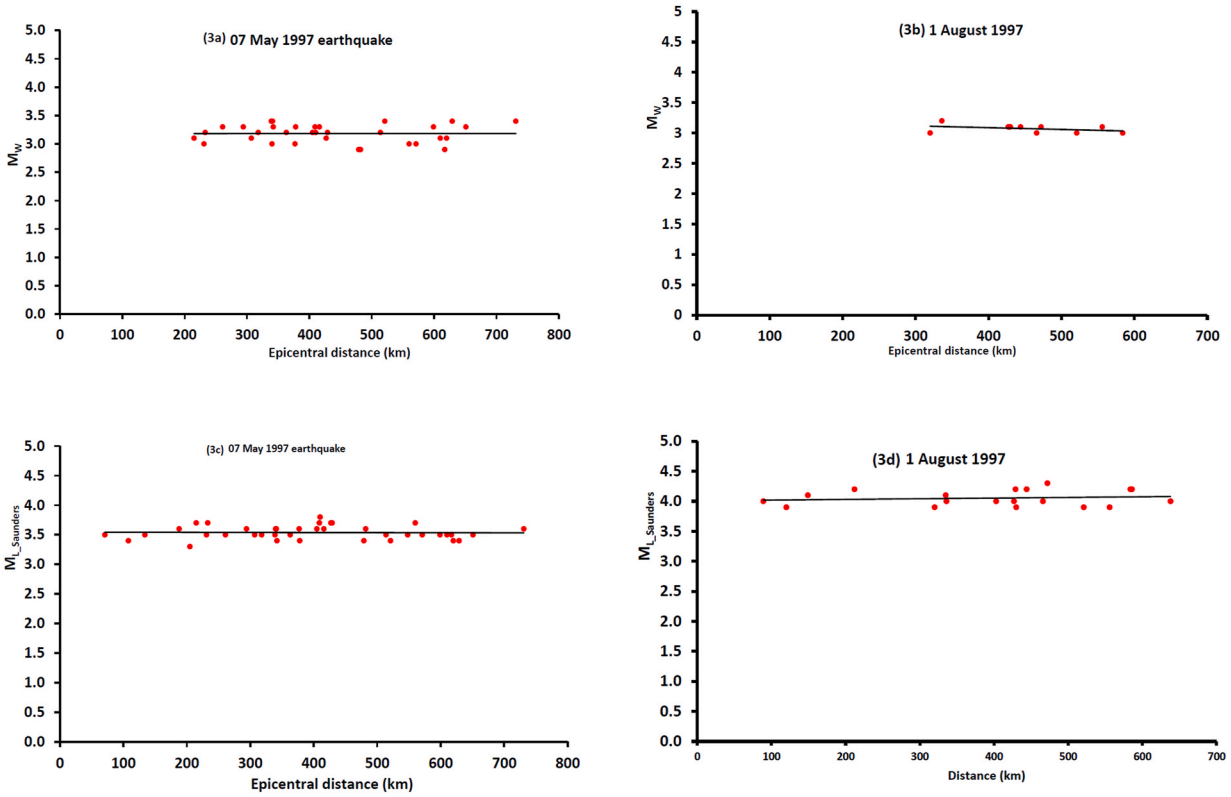

Fig. 3. Variations of M_W and M_L with epicentral distances for two earthquakes that occurred on 7 May 1997 and 1 August 1997. Figures a and b show variations of M_W for both earthquakes, while Figures c and d show the variation of M_L with epicentral distance for the same events. The solid line represents the trend or mean magnitude value. The M_L used in this figure is from the relation by Saunders et al. (2013).

vertical component, R (km) is the hypocentral distance and S is the station correction term. The amplitude is measured after removing the instrument response, which takes the instrument gain into account (Ottemöller et al., 2018).

Given the complexity of determining M_W, an alternative approach is to develop a relation between M_W and the locally developed M_L. This relation would then be used for homogenizing the local catalogue prior to hazard analysis. To do this, earthquakes with magnitudes calculated using both M_W and M_L scales are selected and used to derive regression equations. However, it must be noted that the introduction of the conversion relation will also add uncertainty to the resulting M_W. It is therefore imperative that, when developing the M_W–M_L relation, uncertainty should be assessed and accounted for (Das et al., 2018). The relationship between M_W and M_L scales is of paramount importance for conversions in order to carry out the homogenization of seismicity catalogues for further studies related to seismological statistics. The conversion used to compensate for parameter incompatibilities is usually an aleatory variability, given that M_W and M_L are generally not perfectly correlated (Das et al., 2013, 2018).

Such M_W–M_L relations have been derived for many different regions (e.g. Chavez and Priestley, 1985; Ekström and Dziewonski, 1988; Chen and Chen, 1989; Ambraseys, 1990; Papazachos et al., 1997; Margaris and Papazachos, 1999; Baba et al., 2000). Grünthal et al. (2009a) derived relations between M_W and M_L magnitude scales based on the chi-square maximum likelihood regression technique, with uncertainties given by the 68% confidence bounds. This is a technique that considers errors of individual data points (Stromeyer et al., 2004). Hussein et al. (2008) used linear regression relations between different magnitude scales using relevant statistical parameters, which were derived using orthogonal regression, to convert all the other magnitude scales to M_W.

The derivation of regression relations for M_W and M_L requires that a well-calibrated seismic network correlates M_W estimates with M_L determinations (Ambraseys, 1990; Ekström and Dziewonski, 1988), which is often lacking in regions of low seismicity. A selection of well-recorded events with a good signal-to-noise ratio can be used to model the spectral parameters of the earthquakes in order to derive M_W values (Ottemöller and Havskov, 2003). This process is rigorous and requires high-quality waveform data.

In regions where M_W is reported for very few events, the regression process becomes more complex. In most studies, the calibration earthquakes are selected from global datasets, mostly comprising moderate-to large-magnitude events (Baruah et al., 2012; Das et al., 2014; Grünthal et al., 2009b; Papazachos et al., 1997; Scordilis, 2006).

2. Moment magnitude calculation

The calculation of the moment magnitude, normally derived from the source function of the seismic source spectra, is not a straightforward procedure. In their calculation, Ottemöller and Havskov (2003) applied

the far field source function using Brune's ω^2 model for both P- and S-waves to determine the seismic moment M_0. The source function S(f) for a simple ω^2 model, as defined by Brune (1970; 1971), is given by:

$$S(f) = \frac{M_0\sqrt{0.6\ x\ 2.0}}{4\pi\rho v^3}\left[1+\frac{f^2}{f_c^2}\right]^{-1} \quad (4)$$

where M_o (Nm) is the seismic moment, ρ (kgm^{-3}) is the density, v (km/s) is the S-wave velocity at the source and f_c (Hz) is the corner frequency. For $f < f_c$ the source-amplitude spectrum is flat and proportional to the seismic moment and decays proportional to ω^2 for $f > f_c$. Thus, M_o can be easily determined from the long-period part of the source spectrum (Ottemöller and Havskov, 2003). The moment magnitude scale is then linked to the seismic moment through the linear relation of energy and magnitude, as previously defined by Kanamori (1977).

$$M_w = \frac{2}{3}\log Mo - 6.07 \quad (5)$$

In this study, M_W was determined using the S/Lg wave spectrum on the vertical component of the seismograph following the routine data processing prescribed by Ottemöller and Havskov (2003). Of importance is the region-dependent attenuation function, which needs to be taken into account during the calculation of the M_0, as discussed in Ottemöller and Havskov (2003). The attenuation function is used to determine the source function from the amplitude function (equation (4)). Brandt (2016; 2017a; 2017b) worked extensively to derive the parameters of the attenuation function for different environments within South Africa. They obtained a Q_o value of 391 ± 130 and the near-surface attenuation parameter, Kappa, for mining-related and tectonic events as 0.05 and 0.02, respectively.

3. Data sources and analysis

Spectral analysis was performed on waveform records of 101 seismic events recorded by a temporary network of stations set up during the South African seismic experiment (SASE) project from 1997 to 1999 (Fig. 1). The events had small to moderate magnitude values (M_L between 2.5 and 4.6) and were from mining as well as tectonic sources. No distinction was made between anthropogenic and natural events in this study as it was assumed that the measure of the event was unrelated to its origin. The dataset consists of continuous seismic waveforms at 100 samples per second in miniseed format, from more than 80 stations (Wright et al., 2003). All the selected events fulfilled the requirement of having at least four stations recording the S/Lg waves with a good signal-to-noise ratio to identify, from the displacement spectrum, the low-frequency plateau, the corner frequency and the decay rate for frequencies higher than f_c (Fig. 2). In this study, a good signal-to-noise ratio was taken as 1.5, as suggested by Diehl and Kissling (2007). The spectral analysis for the determination of M_W was done using the SEISAN software package (Ottemöller et al., 2018).

Fig. 2 depicts a typical example of the seismic signals as recorded by the seismographs and its source spectrum. For each station, a window was selected containing S and Lg waves (Fig. 2a) and a spectral analysis was computed on this window to obtain the source parameters (Fig. 2b). The seismic moment, source radius, corner frequency and moment magnitude were calculated. Although some of the events considered in this study are mining related, the risk they pose to infrastructure is the same as for tectonic events and mining-related events are more common (Durrheim et al., 2006; Midzi et al., 2015). Consequently, no distinction between anthropogenic and natural events was made in this study.

To ensure that only S-waves and the Lg wave group are used in the spectrum analysis, the data were filtered at 0.5 Hz to remove low-frequency Rg waves (Hong and Xie, 2005). The example in Fig. 2 clearly shows that only waveforms where the noise spectral level was very low were used in the analysis (grey trace in Fig. 2b). The process to check the spectral noise level was performed for each station and for every event, to ensure that only good-quality records were kept and used in the analysis.

Saunders et al. (2013) pointed out some variation of the determined station magnitude values in respect of the same earthquake (Fig. 3). These variations are expected because there are several factors that influence the propagation of waves from the source to the site (e.g. the radiation pattern is different for each path; each ray path from the source to the station passes through different geological units and different sites have different responses), thus introducing uncertainty in the determination of earthquake magnitudes. For each event, at least four stations were used to compute the average M_W (Fig. 3). Those stations that did not meet the required criteria (i.e. a flat plateau and a fall within the assessed frequency range) were deleted and if the event had not been detected by at least four stations, it was discarded. Ultimately, an average is used as the final M_W with the standard deviation as the uncertainty or error in the magnitude. The average error for each event is given by the following equation:

$$Error = \frac{\sum|M_W - M_{W_{mean}}|}{N} \quad (6)$$

Likewise, the computation of the average M_L and its error were performed following a similar process (Fig. 3). In order to develop conversion relations, a selected set of seismic events needs to have both M_W and M_L values determined. In this case, three M_L relations were considered. Therefore, for each event analysed in this study, four magnitude values were computed - three were computed using M_L relations that had been used by the SANSN and the M_W (Table 2). The variations in M_W and M_L for each event with distance were analysed (for example, Fig. 3 shows results for two earthquakes that occurred on 7 May 1997 and 1 August 1997). In general, both M_L and M_W values appear to be stable with distance, showing consistency in our magnitude determination and stability in regards to the regional attenuation model used.

The mean magnitude residual for each station was calculated by subtracting the station magnitude from the earthquake average value that was calculated using values from all the stations. The plot of the mean residual values against the epicentral distance for both M_W and M_L, follow the zero baselines closely (Fig. 4). Moreover, the residual values for both M_W and M_L are consistent and distance invariant. They generally range within ±0.2, with only a few stations showing large scatter. The observed trend confirms the conclusion by Saunders et al. (2013) that the relationship between attenuation and hypocentral distance in the region is accurately modelled by the attenuation curve.

Given the changes in the relations used to calculate M_L in South Africa, it became clear that the relations linking M_W to the three different M_L types (i.e. Saunders et al., 2013; Fernandez's (1980) modified equation of the Richter equation; Hutton and Boore, 1987) used in South Africa were necessary. It was then possible to prepare three regression relations that would allow for the conversion of all M_L values in the SANSN catalogue to M_W. M_L values calculated using the Hutton and Boore (1987) equation were observed to be generally higher than those of the other relations. This implies that magnitude values for seismic events that had occurred between 1997 and 2012 were overestimated. Therefore, it follows that if a single conversion relation is used this will have the effect of exaggerating the M_W values during the period under consideration.

Table 2
One hundred and one (101) seismic events analysed for M_W and M_L in this study, where $M_{LSaunders}$, M_{LHandB} and $M_{LRichter}$ refer to M_L values determined using the Fernandez (1980), Hutton and Boore (1987) and Saunders et al. (2013) relations, respectively. *represents fixed depth. T represents tectonic events, while M denotes mining-related events.

ID	Year	Month	Day	Hour	Minute	Second	Latitude	Longitude	Depth (km)	$M_{LRichter}$	$M_{LH\&B}$	$M_{LSaunders}$	M_w	T/M
1	1997	4	18	20	1	27.1	−26.284	27.205	2*	2.5	3.4	2.9	2.6	M
2	1997	4	27	23	43	38.1	−26.971	26.811	2*	2.7	3.3	3	2.8	M
3	1997	5	7	10	4	28.8	−26.524	27.301	2*	3.4	4	3.6	3.3	M
4	1997	5	17	10	32	28.9	−26.470	27.534	2*	2.8	3.4	3.1	2.8	M
5	1997	5	21	16	15	17.7	−26.888	26.795	2*	3.1	3.7	3.4	3.1	M
6	1997	5	23	11	16	29.2	−26.896	26.778	2*	3.4	4	3.7	3.5	M
7	1997	5	23	16	13	53.4	−26.827	26.745	10.9	3.2	3.7	3.4	3.4	T
8	1997	5	26	19	18	36.1	−26.917	26.760	2*	2.9	3.5	3.2	3	M
9	1997	6	6	20	58	24.1	−26.790	26.563	2*	3.1	3.6	3.3	2.9	M
10	1997	6	11	23	49	6.0	−26.765	26.559	2*	3.2	3.7	3.4	3.1	M
11	1997	6	19	22	42	36.4	−26.694	26.361	2*	3	3.6	3.3	2.9	M
12	1997	6	25	19	13	30.2	−26.865	26.633	2*	2.8	3.4	3.1	2.7	M
13	1997	6	28	3	35	28.2	−26.335	27.241	2*	3.4	4	3.6	3.3	M
14	1997	6	29	8	24	48.5	−26.389	27.279	2*	3.4	4.1	3.7	3.2	M
15	1997	7	4	0	48	15.2	−26.711	26.705	2*	2.6	3.2	2.9	2.7	M
16	1997	7	6	1	4	10.2	−26.397	27.393	2*	2.4	2.8	2.6	2.5	M
17	1997	7	9	14	3	14.4	−26.307	27.065	2*	2.4	2.7	2.5	2.5	M
18	1997	7	10	7	23	18.4	−26.935	26.767	5.8	2.9	3.4	3.1	2.9	T
19	1997	7	17	22	24	0.7	−26.709	26.541	2*	3.3	3.7	3.5	3.2	M
20	1997	7	21	8	45	47.8	−27.049	26.855	0*	3.8	4.4	4	3.8	M
21	1997	7	29	11	25	5.4	−27.914	26.908	0.1	3.7	4.4	4	3.7	M
22	1997	8	1	2	17	26.3	−27.668	26.329	2*	3.7	4.4	4	3.4	M
23	1997	8	3	2	17	7.3	−28.029	26.832	9.7	2.8	3.6	3.1	3.1	T
24	1997	8	11	16	30	19.9	−27.890	26.565	10.4	3.2	4	3.5	3.1	T
25	1997	8	25	18	41	14.5	−26.330	28.221	2*	2.9	3.6	3.2	3.2	M
26	1997	9	3	15	0	13.9	−26.438	27.297	2*	3.1	3.9	3.5	3.1	M
27	1997	9	11	1	6	5.5	−20.408	24.708	10*	2.7	3.7	3.1	2.9	T
28	1997	9	13	22	43	31.8	−26.873	26.584	2*	3.3	4	3.6	3.2	M
29	1997	9	17	11	58	15.6	−26.548	27.437	2*	3.2	3.9	3.5	3.2	M
30	1997	9	25	0	5	22.5	−26.439	27.493	2*	4.1	4.8	4.4	3.8	M
31	1997	10	5	19	2	1.2	−26.070	27.052	2*	3.4	4	3.7	3.2	M
32	1997	10	11	20	19	10.2	−26.929	26.797	2*	3.4	4.1	3.7	3.2	M
33	1997	10	20	13	36	6.8	−26.903	26.696	38	3.3	4	3.6	3.8	T
34	1997	10	20	19	20	44.6	−26.357	27.319	7.4	3.4	4.1	3.7	3.8	T
35	1997	10	24	13	41	23.5	−27.207	27.437	0.8	2.8	3.6	3.1	3.1	T
36	1997	11	20	0	31	48.2	−26.483	27.474	9.3	3	3.8	3.4	3	M
37	1997	12	11	5	29	45.6	−26.920	26.793	1.8	4	4.6	4.2	3.9	M
38	1997	12	11	12	24	53.9	−27.029	26.896	0.1	2.7	3.3	3	2.8	M
39	1998	1	13	12	32	5.5	−27.160	27.009	0.9	2.6	3.2	2.9	2.9	M
40	1998	1	17	13	6	42.1	−27.024	26.959	1	3.4	4.2	3.7	3.8	M
41	1998	1	27	20	33	18.4	−30.107	30.466	1.6	2.5	3.9	3.1	3.2	T
42	1998	2	3	16	42	36.7	−27.978	26.715	10	3.1	3.9	3.4	3.1	M
43	1998	2	6	7	22	44.9	−27.030	26.819	2	2.9	3.7	3.3	3.1	M
44	1998	2	6	7	52	39.1	−27.035	26.786	16.6	3.2	4	3.6	3.7	M
45	1998	2	18	7	47	15.7	−27.080	26.847	0	3.3	4	3.6	3.6	M
46	1998	2	20	6	21	12.2	−26.544	27.640	2.8	3.1	3.9	3.5	3.1	M
47	1998	3	5	8	36	40.6	−27.032	26.983	0	3.3	4.1	3.7	3.5	M
48	1998	3	24	11	53	42.9	−27.058	26.946	1.8	3	3.7	3.3	3.2	M
49	1998	3	25	21	10	48.9	−27.123	27.118	0	3.2	4	3.6	3.3	M
50	1998	4	4	0	54	31.1	−27.046	26.994	0	3.7	4.3	4	3.6	M
51	1998	4	6	14	41	2.8	−26.890	26.794	15.7	2.9	3.4	3.1	3.2	M
52	1998	4	24	11	44	5.2	−30.995	20.510	9.4	2.9	3.4	3.1	2.9	T
53	1998	4	26	0	50	25.5	−26.466	27.470	13.5	3.5	4.3	3.8	3.8	M
54	1998	5	17	5	14	13.4	−26.918	26.752	0.8	3.5	4	3.7	3.4	M
55	1998	6	19	11	47	48.2	−28.062	26.871	6	3.1	3.8	3.4	3.4	M
56	1998	7	2	18	32	39.5	−28.116	26.881	18.5	2.5	3.3	2.9	3	M
57	1998	7	6	14	48	30.2	−27.052	26.802	9	3.2	3.6	3.4	3.2	M
58	1998	7	13	7	5	4.7	−28.043	26.776	0.7	3.5	4.2	3.8	3.3	M
59	1998	7	26	12	29	57.5	−28.063	26.879	11.8	3	3.5	3.2	3.2	M
60	1998	7	27	18	56	51.5	−26.445	27.413	5.3	3.1	3.4	3.2	3.2	M
61	1998	8	1	6	33	25.7	−26.330	28.286	3.6	3	3.1	3	3.5	M
62	1998	8	9	6	43	27.1	−26.996	26.797	0	3.5	3.6	3.5	3.6	M
63	1998	8	21	16	10	53.5	−27.009	26.770	5.8	3.8	4.1	3.9	3.7	M
64	1998	8	26	2	54	11.4	−27.023	26.735	5.6	2.8	3.2	3	3	M
65	1998	9	16	7	3	1.3	−28.022	26.927	4.5	3	3.6	3.3	3.4	M
66	1998	9	19	10	32	44.9	−26.946	26.741	9.7	3.4	3.8	3.5	3.4	M
67	1998	9	25	15	51	31.4	−26.978	26.801	3.5	3.7	4.1	3.8	3.7	M
68	1998	10	2	7	35	30.5	−26.494	27.380	7.2	3.7	3.9	3.8	3.4	M
69	1998	10	3	16	24	13.3	−26.981	26.755	3.3	3.4	3.6	3.5	3.3	M
70	1998	10	4	9	46	35.4	−26.954	26.776	6.1	3.5	3.9	3.6	3.2	M
71	1998	10	5	22	40	37.7	−30.961	22.492	20	2.5	2.7	2.6	2.8	T
72	1998	10	7	4	51	2.8	−26.441	27.462	3.7	3.2	3.5	3.3	3.1	M

(*continued on next page*)

Table 2 (*continued*)

ID	Year	Month	Day	Hour	Minute	Second	Latitude	Longitude	Depth (km)	$M_{LRichter}$	$M_{LH\&B}$	$M_{LSaunders}$	M_w	T/M
73	1998	10	13	15	52	40.2	−24.456	30.399	11.2	3.4	4.0	3.6	3.3	T
74	1998	11	14	7	18	58.6	−27.005	26.819	15.7	3.0	3.6	3.3	3.3	M
75	1998	11	17	20	17	59.7	−26.991	26.773	5.6	3.8	4.1	3.9	3.8	M
76	1998	11	18	16	30	6.5	−27.008	26.826	15.5	3.7	4.3	4.0	4.0	M
77	1998	11	19	14	7	42.6	−26.503	27.314	3.1	3.0	3.6	3.2	3.2	M
78	1998	12	1	9	22	49.1	−26.943	26.835	5.7	3.0	3.5	3.2	3.2	M
79	1998	12	1	18	12	17.7	−28.134	26.849	2.8	3.3	3.8	3.5	3.4	M
80	1998	12	5	4	52	44.7	−26.409	27.580	1.3	3.8	4.4	4.0	3.8	M
81	1998	12	15	15	52	32.4	−27.011	26.824	13.9	3.3	4.0	3.6	3.5	M
82	1998	12	16	16	0	3.3	−26.463	27.399	7.5	3.7	4.2	3.9	3.6	M
83	1999	1	7	15	18	55.0	−26.985	26.724	11.7	3.3	3.8	3.5	3.4	M
84	1999	1	12	2	50	23.0	−26.568	27.391	24.5	3.0	3.5	3.2	3.1	M
85	1999	2	4	2	2	19.5	−29.889	26.051	0*	4.3	4.3	3.9	3.5	M
86	1999	2	14	19	47	8.3	−30.498	29.157	30.4	4.2	4.2	3.7	3.8	T
87	1999	2	26	9	27	49.8	−26.522	27.399	20.2	3.7	3.7	3.4	3.7	T
88	1999	3	18	11	24	13.0	−26.534	27.391	17.9	4.1	4.1	3.8	4.1	T
89	1999	3	18	17	35	39.3	−26.504	27.356	15.8	3.8	3.8	3.5	3.7	T
90	1999	4	22	22	19	39.0	−28.099	26.587	0.1	4.6	4.6	4.5	4.6	M
91	1999	4	28	15	0	13.4	−26.997	26.997	10*	3.4	3.4	3.2	3.6	T
92	1999	5	10	19	55	42.3	−26.750	27.097	10*	3.9	3.9	3.6	4.1	T
93	1999	5	28	0	16	49.0	−26.791	27.069	10*	3.2	3.2	2.8	3.3	T
94	1999	6	4	8	45	38.4	−27.929	26.779	24.5	3.4	3.4	3.3	3.8	T
95	1999	6	14	15	27	37.9	−26.557	27.620	10*	3.7	3.7	3.4	3.5	T
96	1999	6	24	17	31	58.6	−27.035	26.809	12.6	3.2	3.2	3.0	3.2	T
97	1999	6	24	22	10	29.6	−28.116	26.766	0.1	3.3	3.3	3.2	3.3	M
98	1999	6	25	15	38	46.8	−25.612	30.330	10.6	3.5	3.5	2.9	3.1	T
99	1999	6	30	3	34	44.2	−28.129	26.768	0*	3.4	3.4	3.2	3.3	M
100	1999	6	30	3	41	42.3	−28.050	26.630	0*	3.0	3.0	2.9	2.8	M
101	1999	7	3	20	53	4.0	−29.617	−29.617	24.1	3.8	3.8	3.7	4.0	T

4. M_W–M_L relations

Homogeneity of earthquake data is considered one of the primary requirements for an earthquake catalogue, especially when used for seismic hazard assessment. It is important to know how different magnitude scales compare with one another (Kagan, 2003). Relations between moment magnitude M_W and the three common M_L scales that have been used so far in the South African catalogue were developed. Since both types of magnitudes, as reported in the catalogue, entail uncertainty, the usual meaning associated with "dependent" and "independent" variable fail. Hence, the regression technique to be used should take both sets of errors into account. Standard linear regressions

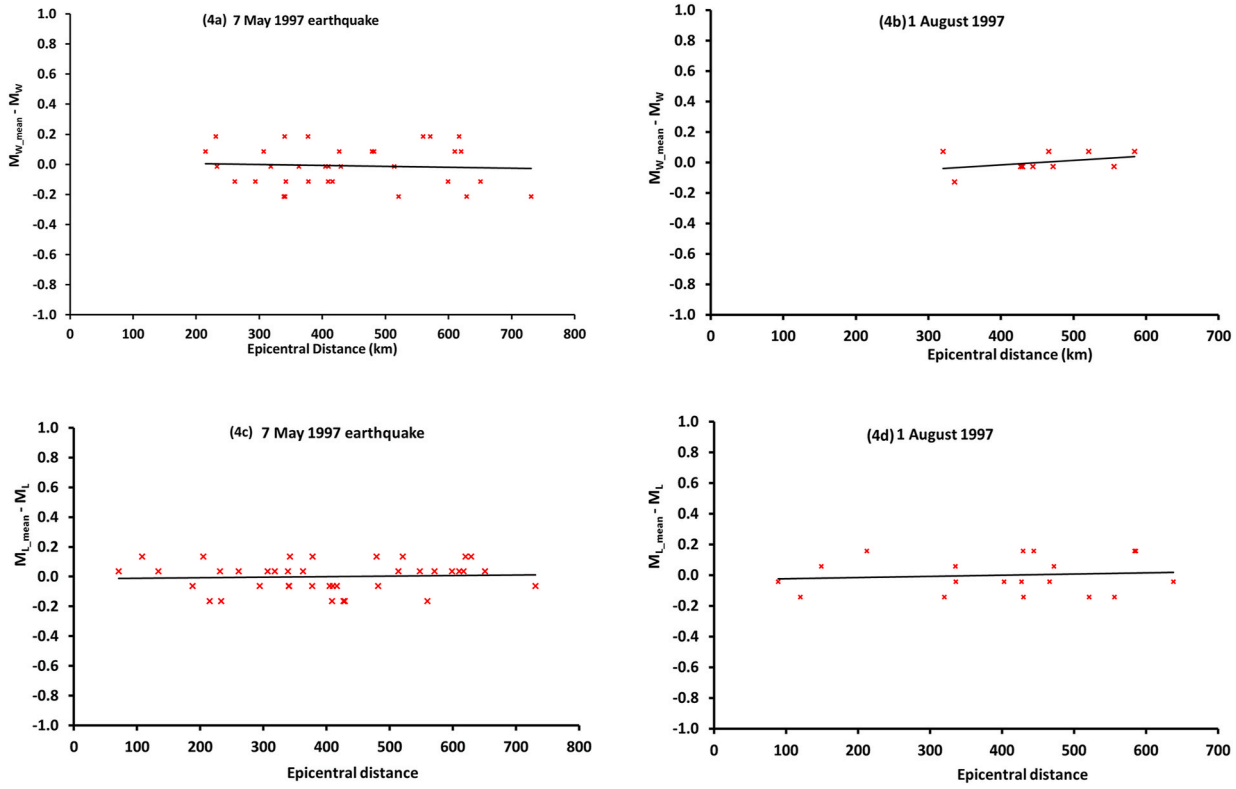

Fig. 4. Mean M_L and M_w magnitude residuals with distance for 1 August 1997 and 7 May 1997 events. M_{L_mean} is the average M_L for the event while M_L represents the M_L at a specific station. Similarly M_{W_mean} is the average M_W for the event while M_W represents the M_W at a specific station. The solid line shows that trendline for the residuals for all magnitudes is almost at zero.

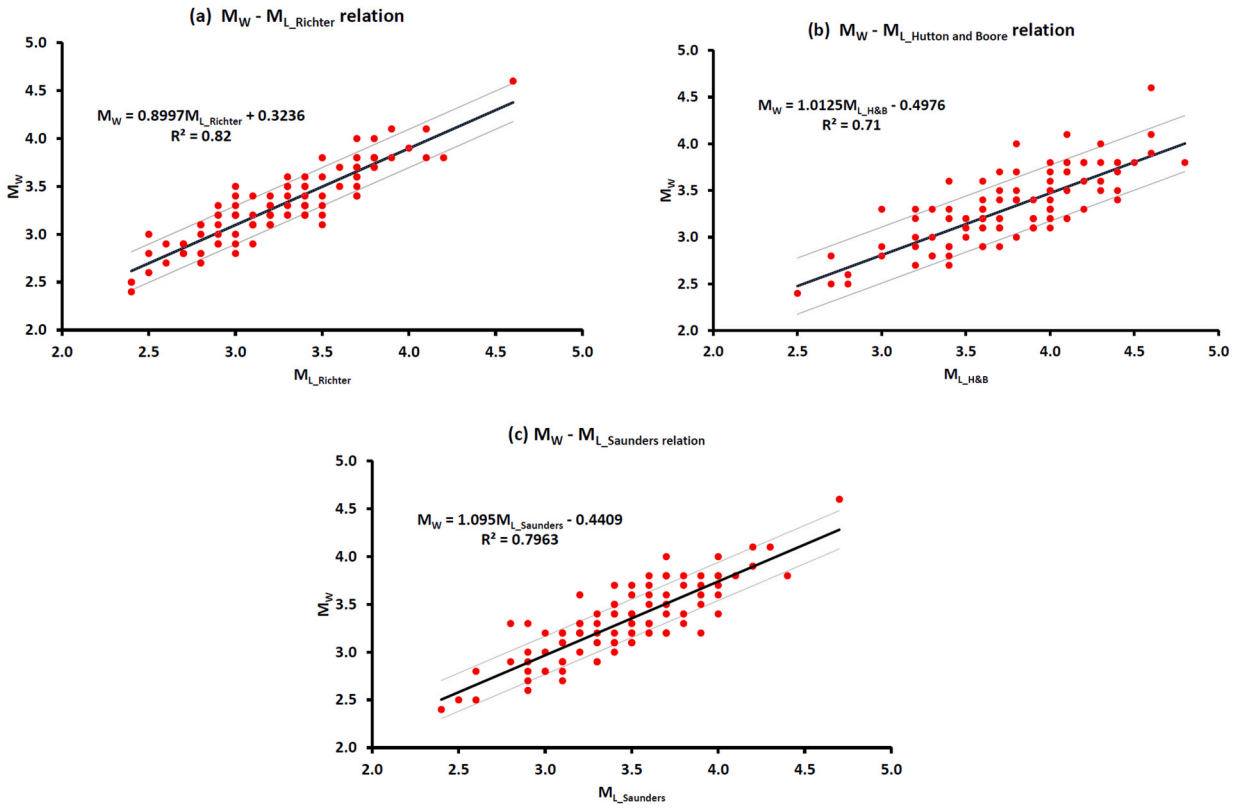

Fig. 5. Results of GOR analysis of moment magnitude (M_W) calculated in this study and the local magnitudes (M_L) used by the SANSN for the compiled dataset, as shown in Table 2. (a) Comparison of M_W to M_L as derived using the modified Richter relation (Fernandez, 1980), (b) Comparison of M_W–M_L, as derived using the Hutton and Boore (1987) relation, (c) Comparison of M_W–M_L as derived using the Saunders et al. (2013) relation. The grey lines represent the uncertainty limits.

Table 3
Derived M_L–M_W relations and their periods of validity for homogenization.

Equation	Homogenization period	Comments
$M_W = 0.8997M_{L\_Richter} + 0.3236$	1970–March 1997	Modified Richter relation (Fernandez, 1980).
$M_W = 1.0125M_{L_{HuttonandBoore}} - 0.4976$	April 1997–September 2012	Derived for Southern California by Hutton and Boore (1987)
$M_W = 1.0957M_{L\_Saundersetal} - 0.4409$	October 2012–present	M_L derived from South African data by Saunders et al. (2013)

assume that the independent variable is either error free or that its error is very small compared to the error of the dependent variable, which makes the technique inappropriate for the derivation of relations for magnitude conversion. On the other hand, the generalized orthogonal regression (GOR) technique takes into account the measurement errors on both linearly related variables. In other words, this technique minimizes the orthogonal residuals for both variables obtained from their orthogonal projections on the GOR line (Das et al., 2011, 2012, 2013, 2018). This technique was used for the inversion of the M_W–M_L relations since both estimates of M_L and M_W are subject to measurement and modelling errors. To compute the regression relations, 85 seismic events selected from Table 2 (event ID 1–85) were used, while the other 16 seismic events (event ID 86–101) were kept in order to test the reliability of our regression equations. Fig. 5 lists the results of the regression analysis.

The three regression relations obtained are shown in equations (7)–(9).

$$M_W = 0.8997M_{L\_Richter} + 0.3236 \pm 0.253 \quad (7)$$

$$M_W = 1.0125M_{L_{HuttonandBoore}} - 0.4976 \pm 0.329 \quad (8)$$

$$M_W = 1.0957M_{L\_Saundersetal} - 0.4409 \pm 0.187 \quad (9)$$

The scatter in the observed data indicates the uncertainties associated with the derivation of the relations. The three regression equations were computed with high R^2 values showing the relative confidence in the equations. The modified Richter relation has the highest R^2 value, while Hutton and Boore's (1987) relation has the lowest. The three equations yield different M_W results for the same M_L and therefore each equation should be used for its period of validity. This exercise highlights the weakness of applying a single global relation to the South African datasets (Bommer et al., 2015; Midzi et al., 2020). Table 3 shows the times of validity suggested for these derived equations, which are the periods of their application in any homogenization process for South African seismic data produced by the CGS. The data used in this study are for magnitudes between 2.5 and 4.6 and, hence, represent the magnitude range for the conversion with high confidence. However, this is also the magnitude range where most seismic events in South Africa

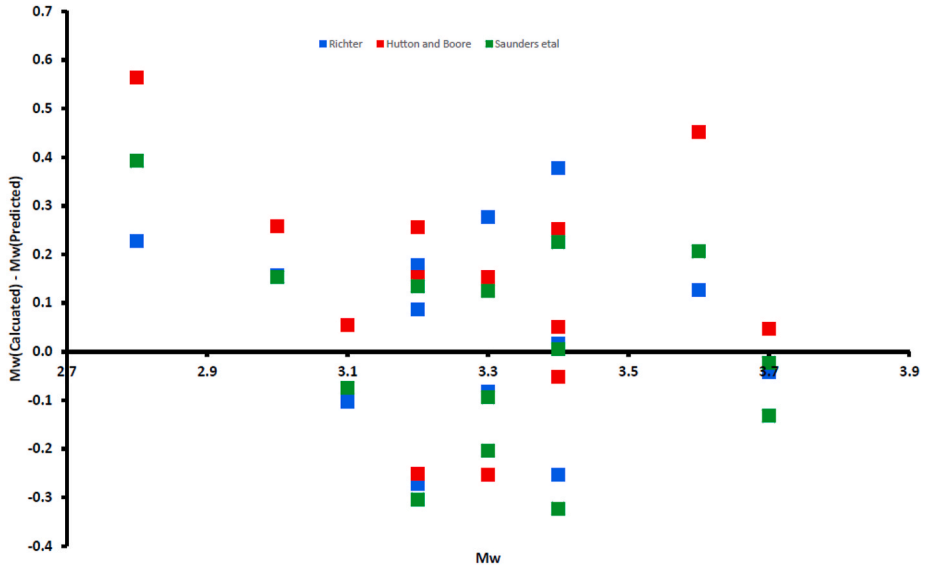

Fig. 6. Comparison of M_w calculated in this study and results predicted by the three magnitude relations computed in this study for the 15 seismic events used in the test.

Table 4
Seismic events with moment magnitude determined by agency Pretoria (PRE) and the Havard CMT. Events in the catalogue region with direct estimates of M_W. The equation number is in brackets. Equation (6) is applied to events prior to 1997. Equation 7 is applied to events between 1997 and 2011. Equation 8 is applied to events after 2012.

Event	M_W (Havard CMT)	M_L (PRE)	M_W (Equations – This study)
01/07/1976 Koffiefontein	5.8	5.8	5.5 (6)
05/01/1986 Matatiele region	5.3	5.1	4.9 (6)
26/09/1990 Welkom	5.0	4.8	4.6 (6)
03/11/1990 Mozambique	5.1	4.9	4.7 (6)
22/02/2006 Mozambique	7.0	7.2	6.8 (7)
23/02/2006 Mozambique	5.7	6.3	5.9 (7)
23/02/2006 Mozambique	5.1	5.4	5.0 (7)
15/03/2006 Mozambique	5.1	6.0	5.6 (7)
15/03/2006 Mozambique	5.6	5.3	4.9 (7)
19/03/2006 Mozambique	4.8	5.2	4.8 (7)
22/03/2006 Mozambique	5.2	6.1	5.7 (7)
23/03/2006 Mozambique	4.8	5.1	4.7 (7)
14/04/2006 Mozambique	5.2	6	5.6 (7)
12/05/2006 Mozambique	4.9	5.8	5.4 (7)
08/06/2006 Mozambique	4.8	5.2	4.8 (7)
30/06/2006 Mozambique	5.0	6.0	5.6 (7)
11/07/2006 Mozambique	4.9	5.3	4.9 (7)
23/08/2006 Mozambique	5.0	5.5	5.1 (7)
20/11/2006 Mozambique	5.1	6.0	5.6 (7)
29/11/2007 Mozambique	5.2	6.2	5.6 (7)
03/02/2008 Mozambique	5.1	6.1	5.7 (7)
05/08/2014 Orkney	5.2	5.5	5.6 (8)
22/09/2016 Mozambique	5.6	5.5	5.7 (8)
03/04/2017 Botswana	6.5	6.5	6.5 (8)

occur.

We tested the regression equations twice. First, 16 selected seismic events (events 86–101 in Table 2) were used to compare the performance of the newly developed relations. The three new relations were used to calculate M_w values for each earthquake and these were then compared to the M_w value determined using spectral analysis and shown in Table 2. Observed residual values from the comparison were less than 0.5 for the Saunders et al. (2013) and Fernandez (1980) relations while the Hutton and Boore (1987) residuals were as high as 0.6 (Fig. 6). This shows that the three relations are stable for homogenizing our catalogue.

In the second test, a set of 24 seismic events, with M_W determined by the Harvard CMT (Ekström et al., 2012), was compared with results derived from the three regression equations (Table 4). This procedure was performed only to obtain insight on how our derived relations compare with the values determined by the Harvard CMT. Each relation was applied to events that occurred during its time of validity. However, a major limitation is that there are very few events with CMT solutions. Results show that the Hutton and Boore (1987) relation (Equation (7)) generally gives values higher than the CMT results, while those from the Saunders relation (Equation (8)) are comparable to the Harvard values. The observed differences may be ascribed to the propagation of uncertainties from the initial M_L scale.

Generally, the M_W computed from the regression equations are comparable to the CMT solutions. The fact that these regression equations give slightly different results for the same event shows why it is important to use them for the correct time period. Residual analysis shows that the equations mostly overestimate in cases where the residuals are higher than 0.4 (Fig. 7). However, there is evidence that uncertainty is reduced when all the seismic events are compared.

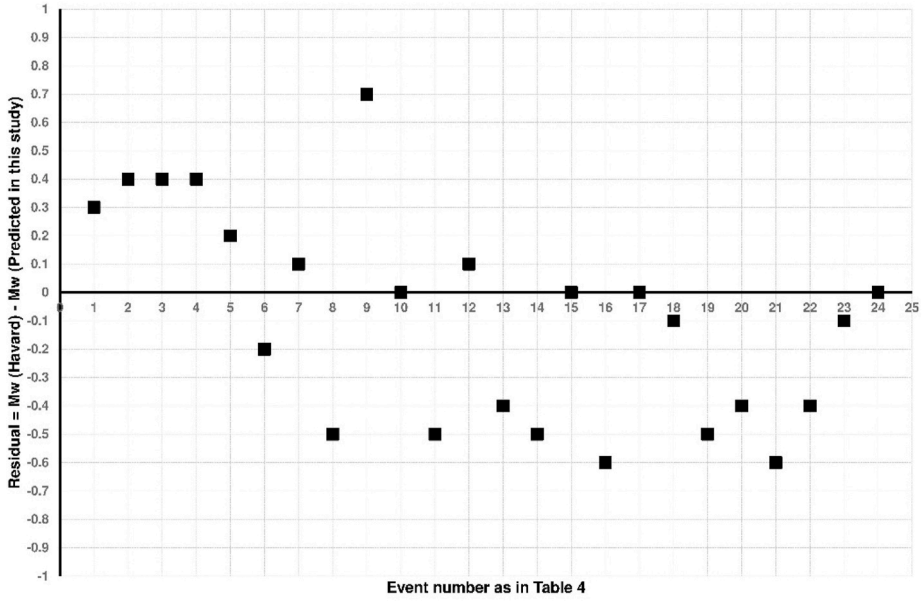

Fig. 7. Comparison of M_w published by Havard CMT and those predicted by the three magnitude conversion relations computed in this study for the 24 seismic events (Table 4).

5. Conclusions

Three M_W–M_L conversion relations were developed using South African data for the homogenization of the SANSN database. The three relations were computed from high-quality data used to compute both M_L and M_W for each event. The moment magnitude was calculated using the S/Lg wave spectra for 101 seismic events recorded by the SASE stations and located in mining and tectonic regions. A minimum of four stations were used to compute the magnitudes and for the error analysis. The GOR method was then used to derive the relations. We show that the assumption that a single magnitude conversion relation can homogenize all events with M_L values in the South African catalogue is not valid (Midzi et al., 2020; Bommer et al., 2015). The results of this work facilitate a reliable homogenization of the South African catalogue from M_L to M_W for events from 1970 to the present, making the method suitable for use in seismic hazard studies in the country. The homogenization process followed in this study assists in the assessment and reduction of the uncertainty and errors associated with new M_W values. In previous attempts to homogenize the catalogue, relations from other regions were utilized (Bommer et al., 2015; Midzi et al., 2020) with the process often resulting in the propagation and amplification of error values. It was shown that there are significant differences between the M_L relations used by the SANSN from 1970 to the present. The application of a single global relation to the SANSN catalogue is certainly not scientifically rigorous. The process of calculating magnitude values is associated with inherent errors and it is therefore prudent to reduce the propagation of these errors in the catalogue homogenization. The M_L relations previously used by the CGS (i.e. the modified Richter scale and the Hutton and Boore (1987) scale) were not derived using South African data and hence they cannot be equated with the Saunders et al. (2013) relation. A comparison of M_W values previously computed by Havard CMT with those computed using the magnitude conversion relations derived in this study produced low residual values, indicating the reliability of the conversion relations.

Declaration of competing interest

The authors declare that they have no known competing financial interests or personal relationships that could have appeared to influence the work reported in this paper.

Acknowledgements

The authors are grateful for the assistance given by Ms Zahn Nel in proofreading our manuscript. The Council for Geoscience very kindly allowed us to use data from their various databases. The authors are also very grateful for the insightful reviews given by the two anonymous reviewers.

Appendix A. Supplementary data

Supplementary data related to this article can be found at https://doi.org/10.1016/j.jafrearsci.2020.104051.

References

Aki, K., 1966. Generation and propagation of G waves from the Niigata earthquake of June 16, 1964, 44. *Bulletin of Earthquake Research Institute (Tokyo University)*, pp. 23–88.

Ambraseys, N.N., 1990. Uniform magnitude re-evaluation of European earthquakes associated with strong-motion records. Earthq. Eng. Struct. Dynam. 19 (1), 1–20. https://doi.org/10.1002/eqe.4290190103.

Baba, A.B., Papadimitriou, E.E., Papazachos, B.C., Papaioannou, C.A., Karakostas, B.G., 2000. Unified local magnitude scale for earthquakes of South Balkan area. Pure Appl. Geophys. 157 (5), 765–783. https://doi.org/10.1007/PL00001117.

Baruah, S., Baruah, S., Kalita, A., Biswas, R., Gogoi, N., Gautam, J.L., Kayal, J.R., 2012. Moment magnitude–local magnitude relationship for the earthquakes of the Shillong–Mikir plateau, Northeastern India Region: a new perspective. Geomatics, Nat. Hazards Risk 3 (4), 365–375. https://doi.org/10.1080/19475705.2011.596577.

Biswas, N.N., Aki, K., 1984. Characteristics of coda waves: central and southcentral Alaska. Bull. Seismol. Soc. Am. 74 (2), 493–507.

Bommer, J.J., Coppersmith, K.J., Coppersmith, R.T., Hanson, K.L., Mangongolo, A., Neveling, J., Stafford, P.J., 2015. A SSHAC level 3 probabilistic seismic hazard analysis for a new-build nuclear site in South Africa. Earthq. Spectra 31 (2), 661–698.

Bormann, P., 2012. New Manual of Seismological Observatory Practice (NMSOP-2), IASPEI, GFZ German Research Centre for Geosciences. https://doi.org/10.2312/GFZ.NMSOP-2. Potsdam.

Brandt, M.B.C., 1997. Implementation of the SEISAN Earthquake Analysis Software for SUN to Analyze the Data Obtained through the South African National Seismograph Network. Council for Geoscience, Pretoria. Report number 1997-0263.

Brandt, M.B.C., 2016. Q_c and Q_S wave attenuation of South African earthquakes. J. Seismol. 20 (2), 439–447. https://doi.org/10.1007/s10950-015-9536-6.

Brandt, M.B.C., 2017a. Near-surface wave attenuation (kappa) of Far West Rand micro-events. J. S. Afr. Inst. Min. Metall 117, 511–516. https://doi.org/10.17159/2411-9717/2017/v117n6a1.

Brandt, M.B.C., 2017b. Near-surface wave attenuation (kappa) of an earthquake near Durban, South Africa. The Southern Afr. Inst. Min. Metall. 117, 1155–1158. https://doi.org/10.17159/2411-9717/2017/v117n12a10.
Brandt, M.B.C., Saunders, I., 2011. New regional moment tensors in South Africa. Seismol Res. Lett. 82 (1), 69–80. https://doi.org/10.1785/gssrl.82.1.69.
Brune, J.N., 1970. Tectonic stress and the spectra of seismic shear waves from earthquakes. J. Geophys. Res. 75 (26), 4997–5009.
Brune, J.N., 1971. Correction to "Tectonic stress and the spectra of seismic shear waves from earthquakes". J. Geophys. Res. 76, 5002. https://doi.org/10.1029/JB076i020p05002.
Burton, P.W., Xu, Y., Qin, C., Tselentis, G.A., Sokos, E., 2004. A catalogue of seismicity in Greece and the adjacent areas for the twentieth century. Tectonophysics 390 (1–4), 117–127.
Castellaro, S., Mulargia, F., Kagan, Y.Y., 2006. Regression problems for magnitudes. Geophys. J. Int. 165 (3), 913–930. https://doi.org/10.1111/j.1365-246X.2006.02955.x.
Chavez, D.E., Priestley, K.F., 1985. M_L observations in the great basin and M_0 versus M_L relationships for the 1980 Mammoth lakes, California, earthquake sequence. Bull. Seismol. Soc. Am. 75 (6), 1583–1598.
Chen, P., Chen, H., 1989. Scaling law and its applications to earthquake statistical relations. Tectonophysics 166 (1–3), 53–72. https://doi.org/10.1016/0040-1951(89)90205-9.
Das, R., Wason, H.R., Sharma, M.L., 2011. Global regression relations for conversion of surface wave and body wave magnitudes to moment magnitude. Nat. Hazards 59 (2), 801–810.
Das, R., Wason, H.R., Sharma, M.L., 2012. Homogenization of earthquake catalog for northeast India and adjoining region. Pure Appl. Geophys. 169 (4), 725–731. https://doi.org/10.1007/s00024-011-0339-6.
Das, R., Wason, H.R., Sharma, M.L., 2013. General orthogonal regression relations between body-wave and moment magnitudes. Seismol Res. Lett. 84 (2), 219–224.
Das, R., Wason, H.R., Sharma, M.L., 2014. Unbiased estimation of moment magnitude from body- and surface-wave magnitudes. Bull. Seismol. Soc. Am. 104 (4), 1802–1811. https://doi.org/10.1785/0120130324.
Das, R., Wason, H.R., Gonzalez, G., Sharma, M.L., Choudhury, D., Lindholm, C., Roy, N., Salazar, P., 2018. Earthquake magnitude conversion problem. Bull. Seismol. Soc. Am. 108 (4), 1995–2007.
Diehl, T., Kissling, E., 2007. User's Guide for Consistent Phase Picking at Local to Regional Scales. Institute of Geophysics. Eidgenössische Technische Hochshule, Zurich, Switzerland, p. 21.
Di Giacomo, D., Bondár, I., Storchak, D.A., Engdahl, E.R., Bormann, P., Harris, J., 2015. ISC-GEM: global Instrumental Earthquake Catalogue (1900–2009), III. Re-computed MS and mb, proxy MW, final magnitude composition and completeness assessment. Phys. Earth Planet. In. 239, 33–47.
Durrheim, R.J., Anderson, R.L., Cichowicz, A., Ebrahim-Trollope, R., Hubert, G., Kijko, A., McGarr, A., Ortlepp, W.D., Van der Merwe, N., 2006. The risks to miners, mines and the public posed by large seismic events in the gold mining districts of South Africa. In: Hadjigeorgiou, J., Grenon, M. (Eds.), Proceedings of the Third International Seminar on Deep and High Stress Mining, 2-4 October 2006, Quebec City, Canada, Université Laval (Canada).
Ekström, G., Dziewonski, A.M., 1988. Evidence of bias in estimations of earthquake size. Nature 332 (6162), 319–323. https://doi.org/10.1038/332319a0.
Ekström, G., Nettles, M., Dziewonski, M., 2012. The global CMT project 2004–2010: Centroid-moment tensors for 13,017 earthquakes. Phys. Earth Planet. In. 200–201, 1–9. https://doi.org/10.1016/j.pepi.2012.04.002.
Fernandez, L., 1980. Adaptation of the Richter seismic local magnitude scale to South Africa. Geolog. Surv. South Afr. Report number 1980-0175. Pretoria.
Gasperini, P., Lolli, B., Castellaro, S., 2015. Comparative analysis of regression methods used for seismic magnitude conversions. Bull. Seismol. Soc. Am. 105 (3), 1787–1791. https://doi.org/10.1785/0120150018.
Greenhalgh, S.A., Singh, R., 1986. A revised magnitude scale for South Australian earthquakes. Bull. Seismol. Soc. Am. 76 (3), 757–769.
Grünthal, G., Stromeyer, D., Wahlström, R., 2009a. Harmonization check of M_W within the central, northern and northwestern European earthquake catalogue (CENEC). J. Seismol. 13 (4), 613–632. https://doi.org/10.1007/s10950-009-9154-2.
Grünthal, G., Wahlström, R., Stromeyer, D., 2009b. The unified catalogue of earthquakes in central, northern and northwestern Europe (CENEC)-updated and expanded to the last millennium. J. Seismol. 13 (4), 517–541. https://doi.org/10.1007/s10950-008-9144-9.
Gutenberg, B., Richter, C.F., 1944. Frequency of earthquakes in California. Bull. Seismol. Soc. Am. 34, 185–188.
Hanks, T.C., Kanamori, H., 1979. A moment magnitude scale. J. Geophys. Res. 84 (B5), 2348. https://doi.org/10.1029/JB084iB05p02348.
Hong, T.K., Xie, J., 2005. Phase composition of regional seismic waves from underground nuclear explosions. J. Geophys. Res.: Solid Earth 110 (B12).
Hussein, H.M., Abou Elenean, K.M., Marzouk, I.A., Peresan, A., Korrat, I.M., Abu El-Nader, E., El-Gabry, M.N., 2008. Integration and magnitude homogenization of the Egyptian earthquake catalogue. Nat. Hazards 47 (3), 525–546. https://doi.org/10.1007/s11069-008-9237-3.
Hutton, L.K., Boore, D.M., 1987. The M_L scale in southern California. Bull. Seismol. Soc. Am. 77 (6), 2074–2094.
Kadirioğlu, F.T., Kartal, R.F., Kılıç, T., Kalafat, D., Duman, T.Y., Azak, T.E., Özalp, S., Emre, Ö., 2018. An improved earthquake catalogue (M ≥4.0) for Turkey and its near vicinity (1900–2012). Bull. Earthq. Eng. 16 (8), 3317–3338.
Kagan, Y.Y., 2003. Accuracy of modern global earthquake catalogs. Phys. Earth Planet. In. 135 (2–3), 173–209.
Kanamori, H., 1977. The energy release in great earthquakes. J. Geophys. Res. 82 (20), 2981–2987.
Kanamori, H., 1983. Magnitude scale and quantification of earthquakes. Tectonophysics 93 (3–4), 185–199. https://doi.org/10.1016/0040-1951(83)90273-1.
Kim, W., 1998. The M_L scale in eastern north America. Bull. Seismol. Soc. Am. 88 (4), 935–951.
Lay, T., Wallace, T.C., 1995. Modern Global Seismology. Academic Press.
Margaris, B.N., Papazachos, C.B., 1999. Moment-magnitude relations based on strong-motion records *in of the Seismological Society of America*, in Greece. Bull. Seismol. Soc. Am. 89 (2), 442–455.
Midzi, V., Manzunzu, B., Mulabisana, T., Zulu, B.S., Pule, T., Myendeki, S., 2020. Probabilistic seismic hazard maps for South Africa. J. Afr. Earth Sci. 162, 103689.
Midzi, V., Zulu, B., Manzunzu, B., Mulabisana, T., Pule, T., Myendeki, S., Gubela, W., 2015. Macroseismic survey of the M_L 5.5, 2014 Orkney earthquake. J. *Seismol.* 19 (3), 741–751.
Muço, B., Kuka, N., Shubleka, S., 2002. Development of a moment magnitude relation for Albania. Bull. Seismol. Soc. Am. 92 (3), 1136–1140. https://doi.org/10.1785/0120010204.
Nuttli, O.W., 1973. Seismic wave attenuation and magnitude relations for eastern North America. J. Geophys. Res. 78 (5), 876–885.
Ottemöller, L., Havskov, J., 2003. Moment magnitude determination for local and regional earthquakes based on source spectra. Bull. Seismol. Soc. Am. 93 (1), 203–214.
Ottemöller, L., Voss, P., Havskov, J., 2018. SEISAN Earthquake Analysis Software for Windows, Solaris, Linux and Macosx. Bergen. Retrieved from. http://seisan.info.
Papazachos, B.C., Kiratzi, A.A., Karacostas, B.G., 1997. Toward a homogeneous moment-magnitude determination for earthquakes in Greece and the surrounding area. Bull. Seismol. Soc. Am. 87 (2), 474–483.
Saunders, I., Ottemöller, L., Brandt, M.B.C., Fourie, C.J.S., 2013. Calibration of an M_L scale for South Africa using tectonic earthquake data recorded by the South African National Seismograph Network: 2006 to 2009. J. Seismol. 17 (2), 437–451. https://doi.org/10.1007/s10950-012-9329-0.
Scordilis, E.M., 2006. Empirical global relations converting M_S and m_b to moment magnitude. J. Seismol. 10 (2), 225–236. https://doi.org/10.1007/s10950-006-9012-4.
Stromeyer, D., Grünthal, G., Wahlström, R., 2004. Chi-square regression for seismic strength parameter relations and their uncertainties, with applications to M_W an based earthquake catalogue for central, northern and northwestern Europe. J. Seismol. 8, 143–153. https://doi.org/10.1023/B:JOSE.0000009503.80673.51.
Stucchi, M., Rovida, A., Capera, A.G., Alexandre, P., Camelbeeck, T., Demircioglu, M.B., Gasperini, P., Kouskouna, V., Musson, R.M.W., Radulian, M., Sesetyan, K., 2013. The SHARE European earthquake catalogue (SHEEC) 1000–1899. J. Seismol. 17 (2), 523–544.
Wright, C., Kgaswane, E.M., Kwadiba, M.T.O., Simon, R.E., Nguuri, T.K., McRae-Samuel, R., 2003. South African seismicity, April 1997 to April 1999 and regional variations in the crust and uppermost mantle of the Kaapvaal craton. Lithosphere 71 (2–4), 369–392. https://doi.org/10.1016/S0024-4937(03)00122-1.